Tension Technology International, Inc
USA

Tension Technology International, Ltd
UK

REPORT

ANALYSIS OF NON-BUOYANT LOBSTER LINES
NEW, USED AND MACHINE TESTED

Visual Examination
Microscopic Examination
Rope and Yarn Strength Testing
Scanning Electron Microscopy

Prepared for

Massachusetts Division of Marine Fisheries
and
Atlantic Offshore Lobstermen's Association

By

Tension Technology International, Inc.
35 Hubbard Rd
Weston, Massachusetts 02493
USA
Tel: 781 235-1345
e-mail: tti@tensiontech.com

May 17, 2006

1 INTRODUCTION

Regulations are pending that would require non-buoyant lines for offshore lobstering groundlines and other fishing activities that are currently using buoyant lines. The reason is that buoyant lines entangle with whales and vessels when they float above the seabed or break free. Non-buoyant lines on the bottom can become contaminated with sediment which causes internal and external abrasion during handling operations, thus reducing their life or causing the loss of gear if they break.

This is a condensed version of a report submitted to the Massachusetts Division of Marine Fisheries (DMF) and the Atlantic Offshore Lobstermen's Association. The work was part of a program to find and/or develop durable and cost-effective non-buoyant groundlines for use by the offshore lobster industry. Only one specimen, that designated L1 is reported in detail in this abridged report: however, the other specimens showed similar results and some data is cited. The full report may be obtained from TTI at the address on the title page or from the Massachusetts Division of Marine Fisheries, Gloucester, Massachusetts.

Three rope specimens were received from DMF by TTI and were designated L1, L2 and L10. Each specimen was taken from new, used and machine tested ropes. Two were of three strand laid construction and one was four strand. The ropes were made with a combination of polypropylene (PP) fiber, which is buoyant, and polyester (PET), which sinks; the resulting ropes were intended to be barely non-buoyant. The used rope specimens were collected from lobster fishermen after an unspecified time in service. Usage was enough to induce visible abrasion and later testing showed lower strength than the new lines.

The machine tested ropes had been cycled through a machine designed to simulate actual recovery of lobster traps. See footnote[1] for a link to a report that provides a description of the machine, test procedure and test results. A brief description is provided below as a quick reference.

An over all view of the simulator is provided in Figure 1. A hydraulically driven pulley, Figure 2, simulates a typical hauling winch. The pulley develops tension through friction and the wedging action of the Vee shape shown in Figure 3. However, the wedging action creates considerable lateral pressure on the rope. There is also sliding action on the pulley surface as the rope passes around it causing rubbing which is a source of external fiber abrasion.

A brake, also utilizing friction, is located at the opposite end of the machine. See Figure 4; this simulates the weight of the haul. The friction is developed by wrapping several turns around a drum. The helical guides move the rope laterally along the drum. In this case, constant rubbing occurs on the surface of the drum and against the helical guides. The brake creates abnormal surface rubbing but is not considered significant. Test tension was 1160 lbs.

[1] **http://www.mass.gov/dfwele/dmf/programsandprojects/ritwhale.htm#right**

A continuous loop of rope is driven through the machine for a specified time. The upper section between the drive and the brake was taut. The portion below was slack and traveled through a bed of sediment in a water bath. The ropes were tested for strength after the designated running time.

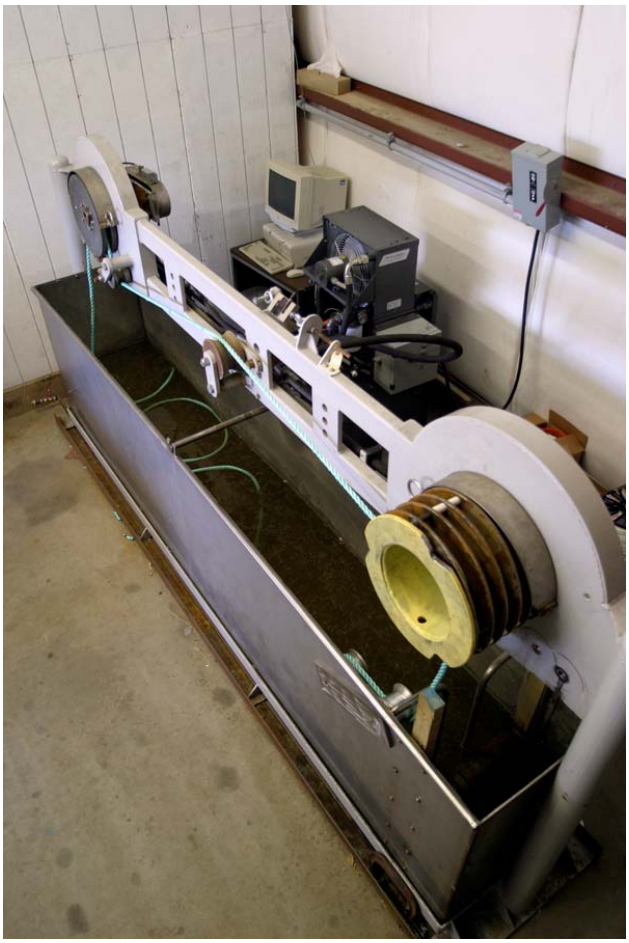

Figure 1 Abrasion simulator for lobster groundlines exposed to bottom sediment and then experiencing hauling operations.

Figure 2 Drive pulley simulating rope hauler.

Figure 3 Vee shape of hauler drive pulley.

Figure 4 Break used to simulate hauling tension.
Tests were run at 1160 lbs tension.

The work performed by TTI in the study was as listed below.

1. Determine the strength of untested specimens and the residual strength of used and machine tested specimens, by performing whole rope and yarn tests. Establish constants for future yarn-to-rope strength conversions for used ropes.
2. Suggest a test method for specific gravity of ropes.
3. Examine wear visually.
4. Examine rope microscopically and identify types of damage.
5. Examine presence of sediment and consider a test to quantify sediment density.
6. Discuss the applicability of the machine test apparatus as a tool for evaluating ropes for non-buoyant lobster line service.
7. Propose a rope construction that would resist sediment contamination and limit its effects.

2 EXECUTIVE SUMMARY

The general conclusions are as stated below.

1. The testing machine appears to reproduce mechanical damage quite well. This is damage caused by external rubbing, pressure (squeezing) and flexing (running over pulleys). It was not possible to quantitatively determine the contribution to damage by the presence of sediment.

2. Particle migration through a rope cross-section was less for machine tested ropes than for used ropes.
3. The sediment concentrations in the ropes were so small that a method of physically collecting them was not considered feasible. Also, sediment is seen to collect in pockets in the scanning electron microscope (SEM) photos, so an average density does not seem useful. The SEM did provide a means to compare sediment concentrations between specimens.
4. External abrasion on both the used and machine tested lines was most likely caused by rubbing due to working the ropes over friction driven winches. The rate of fiber damage was certainly accelerated by the presence of sediment but this could not be quantified.
5. Pressure from the winch drive and flexing over pulleys caused flattening of the filaments of PET yarns, and, splitting, flattening and compression of the PP yarns. These effects were widely observed but cannot be directly attributed to sediment contamination.
6. Internal flex fatigue was evident on the PP monofilaments. Splits were found that suggested a de-lamination process had occurred due to differential stresses within the filament, probably caused by repeated bending and/or elongation.
7. Most internal fiber abrasion was caused by strand-on-strand rubbing which is known to be strongly affected by the presence of sediment particles but could not be observed.
8. Tightly twisted yarns of PET multifilaments in some of the specimens show a low concentration of sediment particles.
9. There was a size difference between the machine sediment medium (up to 100 mμ but mostly less than 10 mμ) and the sediment observed in the used ropes (50 mμ to 100 mμ). Some evidence exists that indicates that smaller particles are more damaging. For reference, PET filament size is about 20mμ and the PP filaments are mostly rectangular about 400 mμ x 200 mμ. The chemistry of the sediment also differed as indicated by X-Ray spectra analysis. It is important to note these variables but we can only speculate on the effect on rope performance for these particular specimens.
10. Strength testing yielded limited useful information. This was due to limited specimen availability. The machine tested specimens could not be tested and a very small number of tests were possible on the others..
11. Strength testing illustrated how yarn testing can be used to evaluate rope condition without having to test a whole rope.

3 DETAILED REPORT

VISUAL EXAMINATION

The visual examination was conducted by dissecting samples down to the rope yarn level and making a photographic record of the condition of the rope, from whole rope to strand to rope yarn. The ‘machine tested’ samples received by TTI were very short, about 3ft in length, and contained various splices. Thus, only a dissection of these samples was possible. The ‘new’ and ‘used’ samples were of sufficient length to permit dissection, strand tensile testing and whole rope tensile testing.

TYPICAL VISUAL ANALYSIS OF SPECIMENS'

The specimens for rope L1 are shown in Figure 5. It was designated as $^{5}/_{8}$ inch diameter [0.625 inches - 16mm] but was undersized as reported in Table 1.

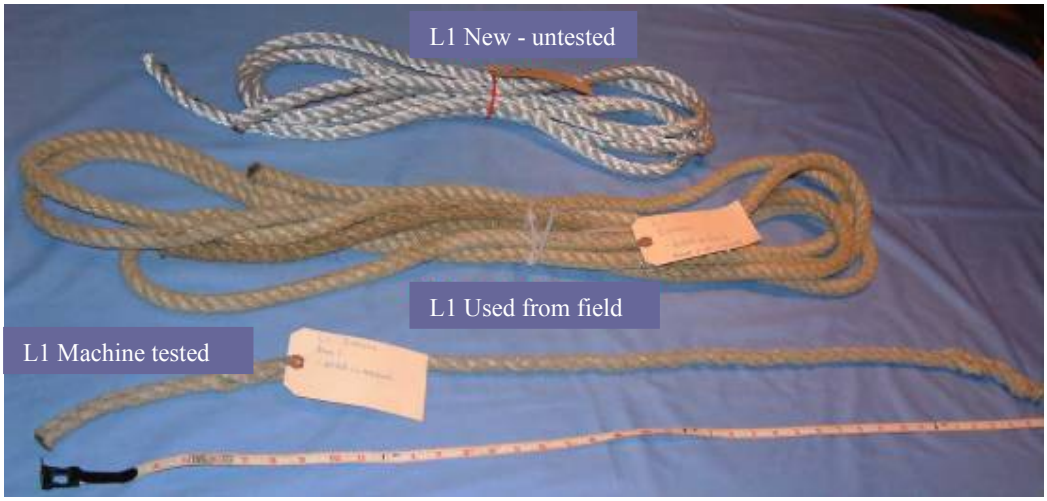

Figure 5 General view of new, used and machine tested samples for L1 rope.

Initial measurements were made on the new rope, and are shown in Table 1.

Table 1. Initial measurements made on Line L1, new [untested].

Reference tension[1]	70.5 lbf [32 kgf]
Measured diameter[2]	0.594in [15.1mm]
Rope lay[3]	2.28in [58mm]
Strand twist[4]	5.88 turns/ft [19.3 turns/meter]
Rope yarns per strand	18, 12 outer and 6 inner. A combination of monofilament and multifilament textile yarns has been used to construct a strand

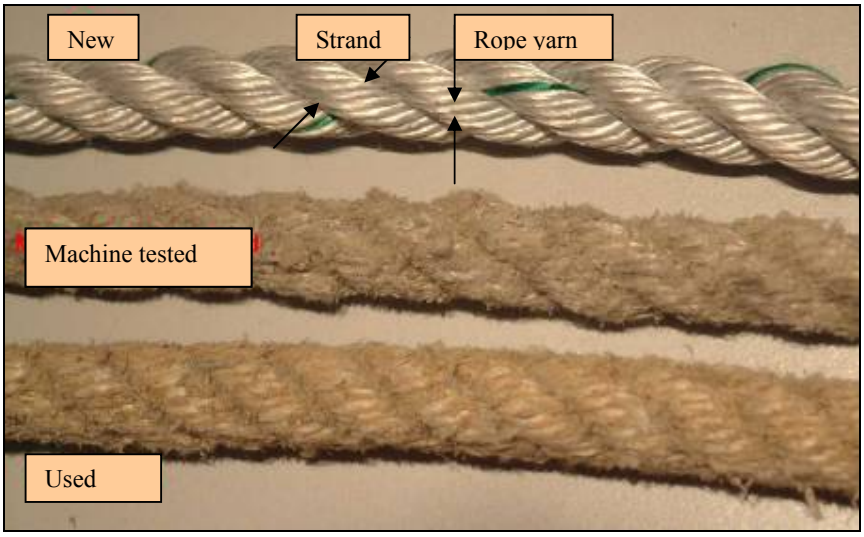

Figure 6 Close view of L1 new, used and machine tested samples.
Note that each strand is constructed from multiple rope yarns.

It may be seen that there is a difference in appearance between the machine tested and used samples, with the machine tested sample appearing to be more abraded.

The strand lay angle for all three specimens is about 33 degrees

Figure 7 L1 View of deconstructed rope specimen into strands, bundles of rope yarns and individual rope yarns.

VISUAL INSPECTION OF L1 USED ROPE

Figure 8 Close view of a used strand

Both external and internal abrasion is seen. Ridge caused by adjacent strand pressure.

Figure 9 L1 Close view of used outer rope yarns

The result of external and internal abrasion is clearly seen. Internal fiber abrasion is less than external

Figure 10 L1 Close view of used inner rope yarns

Photo note: Inner rope yarns are in the center of the stand and do not come to the surface . The condition of these rope inner yarns is clearly better than the outer rope yarns (photo above)

VISUAL INSPECTION OF L1 MACHINE TESTED ROPE

Figure 11 L1 Close view of machine tested strand

Photo note: Both external and internal abrasion damage is seen

Compare to Figure 8 above

Figure 12 L1 Close view of machine tested outer rope yarns

Photo note: Abrasion damage is seen, with one rope yarn completely severed

Figure 13 L1 Close view of machine tested inner rope yarns

When comparing the machine tested (above) and used conditions, photos (figures above) it is seen that the poorer appearance of the machine tested rope is reflected in the higher degree of abrasion damage seen at the rope yarn level. Although the service conditions of the used rope are unknown, it may be speculated that the mechanical effects of the machine testing is more severe.

4 TENSILE TESTING

Whole rope testing was conducted for new and used ropes. The rope samples available for machine tested ropes were too short to prepare test specimens. For yarn strength testing, dissecting the ropes down to their rope yarn or textile yarn level, would be very disruptive of the structure. It was decided to use only dissected strands for this work,

TENSILE RESULTS, STRAND TESTING

Tables 2, 3 and 4 show the tensile results for the strand testing, and Tables 5, 6 and 7 show the results of the whole rope testing.

Table 2

	L1 Everson 'Neutral Buoyancy'					
	Strand 1	Strand 2	Strand 3			
	Br strength kN	Br strength kN	Br strength kN	**Summed Br strength kN**	**Summed Br strength lbf**	**Loss – used summed strength % of untested**
Untested	18.403	19.274	19.237	**56.914**	**12794**	**44.6**
Used	8.897	11.284	11.334	**31.515**	**7085**	

Table 3	L2 4-Strand							
	Strand 1	Strand 2	Strand 3	Strand 4	Core			
	Br strength kN	Br strength kN	Br strength kN	Br strength kN	Br strength kN	**Summed Br strength kN**	**Summed Br strength lbf**	**Loss used summed strength % of untested**
Untested	14.956	15.311	14.545	17.777	4.623	**67.212**	**15109**	**52.8**
Used	8.034	5.443	8.575	7.8021	1.869	**31.7231**	**7131**	

Table 4	L10 Anacko 'Neutral Buoyant'					
	Strand 1	Strand 2	Strand 3			
	Br strength kN	Br strength kN	Br strength kN	**Summed Br strength kN**	**Summed Br strength lbf**	**Loss of summed strength % % of untested**
Untested	19.020	19.016	19.312	**57.348**	**12892**	**42.6**
Used	10.713	10.942	11.236	**32.891**	**7394**	

TENSILE RESULTS, WHOLE ROPE TESTING

In order to make the most efficient use of the available material, it was decided to use a bollard grip system. Figure 14.

Figure 14 Front view of bollard assembly

The diameter of the bollard is 100 mm, 4”

Table 5 Whole rope tensile testing L1 Everson

	Breaking Load kN	**Breaking Load lbf**	**Comment**
Untested	29560	6645	Failure at leading edge of bollard wrapping
Used	22359	5026	Failure clear of bollards
Machine tested	-	-	

Table 6 Whole rope tensile testing L2 4-strand

	Breaking Load kN	**Breaking Load lbf**	**Comment**
Untested	31.534	7089	Failure clear of bollards
Used	18.991	4269	Failure within bollard wrapping
Machine tested	-	-	

Table 7 Whole rope tensile testing L10 Anacko

	Breaking Load kN	**Breaking Load lbf**	**Comment**
Untested	38.255	8600	Failure clear of b bollards
Used	24.998	5620	Failure clear of bollards
Machine tested	-	-	

DISCUSSION OF STRAND AND WHOLE ROPE TENSILE TESTING

The loss of strength cannot be compared between various rope types as the conditions of use of the used specimens is unknown and obviously not the same as the machine tested specimens. However, some useful observations and comparisons can be made.

Whole rope testing had been conducted earlier by two laboratories, NW Labs and Kenney. These data are included for comparison in Table 8. Inter-lab correlation for strength testing of identical ropes is known to have a high variability, but the high Kenny data cannot be explained. Much depends on the termination and/or method of gripping the rope which was unknown.

Table 8 Comparison of whole rope tensile strength results.

		NW Labs			**Kenny**			**TTI**		
	Sample	New Line	Machine Test	% Loss	New Line	Machine Test	% Loss	New Line	No Test	% Loss
Br Load lbf	L1	6400	4571	28.6	9658	5745	40.5	6645	--	--
	L2	8323	4533	45.5	10196	5381	47.2	7089	--	--
	L10	5840	3662	37.3	8938	4182	53.2	8600	--	--

Because of the high new rope strength results from Kenney, this may explain why the % loss of strength results are higher.

Table 9 Summary of strand and whole rope testing conducted by TTI Ltd

Sample	Summed strand Break Strength lbf	Loss of strength, strands %	Whole rope Break strength lbf	Loss of strength, Whole rope %	Calculated Realization Factor
L1 Everson untested	12,794	44.6	6,645	24.2	0.519
L1 Everson used	7,085		5,026		0.709
L2 4-strand untested	15,109	52.80	7,089	39.80	0.469
L2 4-strand used	7,131		4,269		0.599
L10 Anacko untested	12,892	42.6	8,600	34.7	0.667
L10 Anacko used	7,394		5,620		0.760

The table shows the calculation to derive the Realization Factor for each of the rope samples done by dividing the Whole Rope Breaking Strength by the Summed Strand Breaking Strengths. For each pair of ropes, it can be seen that the Realization Factor is greater for the used specimens as compared to the untested specimens.

This comparison is based on limited data, but indicates a trend that is typical for ropes. Whole ropes will break well below the summed yarn strengths. The L1 Everson is a smaller diameter than the others and will have a lower breaking strength on an exponential basis. Yet L1 had the best abrasion performance in machine testing based on NW Labs strength test data.

These results, showing L1 superior, also appear consistent with the abrasion levels seen in the yarn photographs for machine tested ropes.

This result is in line with TTI experience regarding 4-strand constructions used in fishing applications, and TTI would not recommend this particular construction for this application. For example, the smaller strands are likely to loose strength faster.

5 SCANNING ELECTRON MICROSPOY

INTRODUCTION

The general conclusion from the visual examination is that is that both internal and external abrasion are significant factors in the deterioration of the ropes. As both used ropes from the field and machine tested ropes have been subjected to extensive contact with sediment, there remains the question as to what degree the sediment has penetrated the rope structure, and then to what degree has the sediment contributed to the abrasion damage seen.. On dissection of all three ropes, for both conditions, the release of particulate matter was minute. It was decided to use SEM [scanning electron microscopy] to investigate the fatigue damage mechanisms in greater detail, and to assess, by means of visual inspection of the images, the contribution made to the rope damage by the sediment.

The images shown below are compressed JPEG, and are better viewed in Word at 200%.

L1 MACHINE AND USED TESTED COMPARISONS

Figure 15 shows a general view of used and machine tested strands. Note that 'ridge, 'inner face' and 'outer face' are indicated.

Figure 15 L1 General view of used and machine tested strands

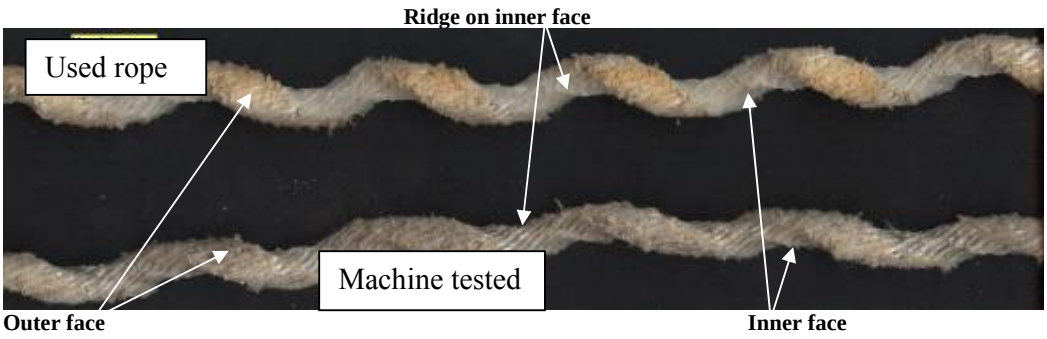

Machine tested

Figure 16 shows a general view at x18 magnification of the outer face of a strand.

Figure 16 L1 Machine Tested -General view, outer face of strand

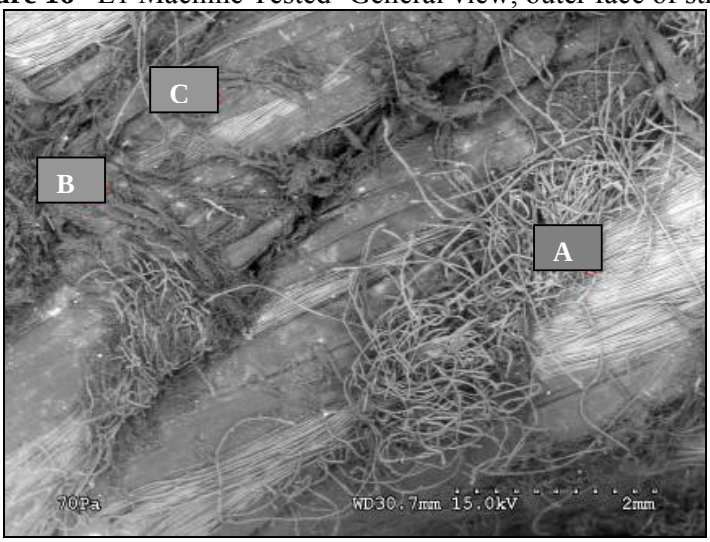

The thick monofilament polypropylene [PP] and fine multifilament polyester [PET] components of the strand are immediately seen. In general, the finer , intact, PET filament material, is lighter in color (naturally white) although the tangled PET filaments appear dark due to contamination, such as rust or dirt.

Broken and tangled PET filaments are obvious. at 'A'. At 'B' there is abraded and fibrillated material, assumed to be from the PP monofilament component. Amongst the filaments, sediment particles may be seen, showing as white dots or spots. From the scale shown on the photograph, the larger particles are about 100 micron, whilst the smallest ones are less than 10 micron.

At ‘C’, there is an example of a monofilament that has been so severely abraded that just a layer of it remains, overlying the PET filaments beneath. The underlying filaments can be seen throughout the remaining PP material.

Figure 17, next page, shows a close view of the abrasion damage to a PP monofilament.

Figure 17 L1 Machine Tested
Close view of abraded PP, outer face of strand

At ‘A’, fibrillated PP material, the result of abrasion, is seen, whilst at’ B’ the remains of a PP monofilament is seen.

The PET filaments appear in reasonable condition, despite the severe damage seen on the PP material. There is some evidence of short grooves on the surface of some of the PET filaments that may well be the result of abrasion caused by particles. The damage to the PP does not appear to have been caused by particles, the more likely source of this damage is surface abrasion caused by winding of the ropes by winches.

Sediment particles, the majority circa 10 micron, are seen on both the PP and PET filaments.

Photographs 18, 19 and 20 show further views of mechanically damaged (external rubbing or flexing) PP and PET material.

Photograph 18 L1 Machine Tested - Close view of damaged PP and PET, outer face of strand

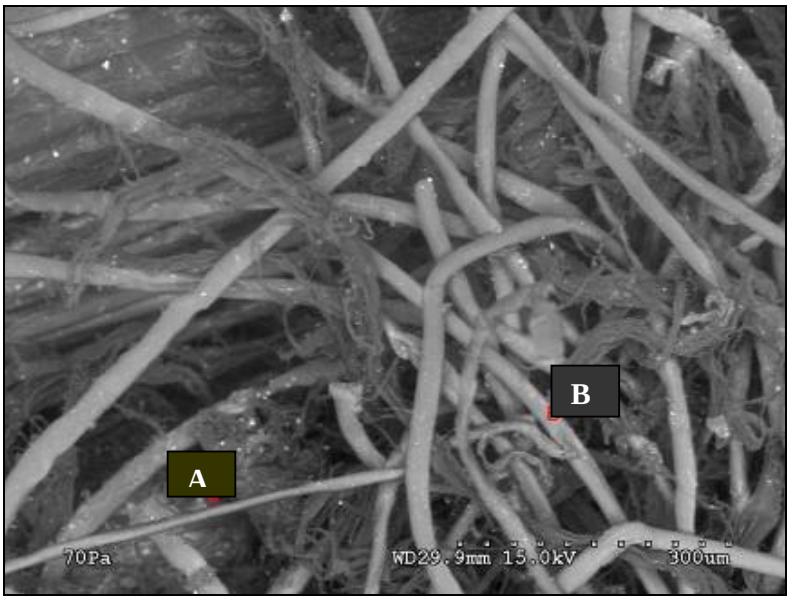

Flattening of the PET filaments is seen on this photograph, as shown at 'A'.

At 'B', there is a large groove on a PET filament. There are no large sediment particles in the vicinity, and this damage is more likely to have been caused by filament-filament abrasion. Fibrillated PP debris [the darker tangled masses] is also in evidence.

Figure 19 L1 Machine Tested - View of outer filament failure B of Photograph 17

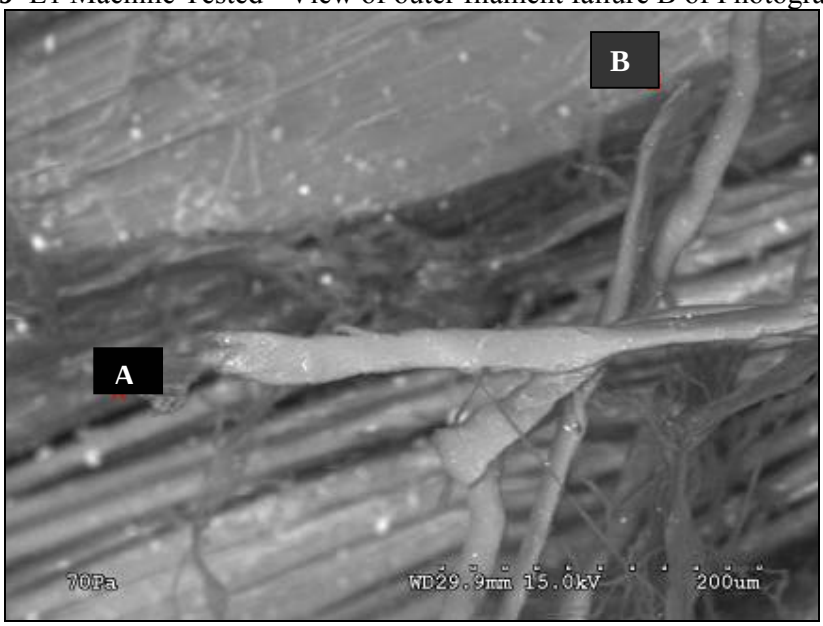

The failed end is clearly seen at 'A', with severe flattening to the upper surface of the filament. At 'B', another failed end is seen, but there appears to be very localized twisting in the failure zone. Flattening of a filament would not be caused by sediment abrasion.

Photograph 20 is of the inner face of a strand. Sediment accumulation would be expected to be more concentrated here as it would not be easily washed off during hauling operations.

Photograph 20 L1 Machine Tested
Close view, inner face of strand

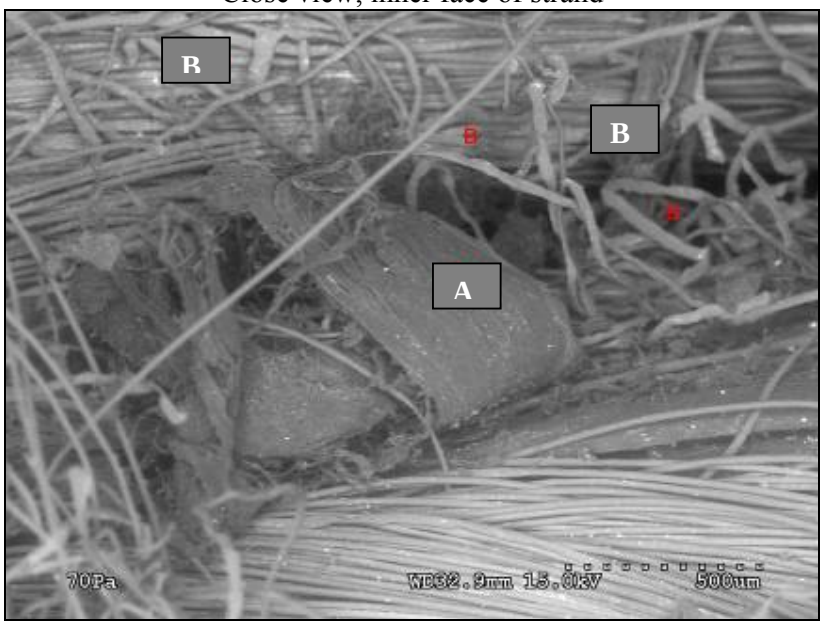

At 'A', the PP filament has partially failed under tension. The result is a lash back mechanism that causes the failed material to be out-of-plane with respect to the remainder of the filament. The partial failure was most likely initiated by localized flex-fatigue of an abraded part of the filament.

Sediment particles are seen throughout the photograph, but particularly on the under-face of the failure 'A'. This is evidence that the filament had suffered surface damage before the particles were present, as there could be no way for them to penetrate the internal structure if the filament surface was undamaged.

Flattened PET filaments are seen at 'B'.

A significant proportion of the PET filaments appear in reasonable condition, as seen to the bottom right hand side of the photograph.

Photograph 21 L1 Machine Tested
General view, strand cross-section

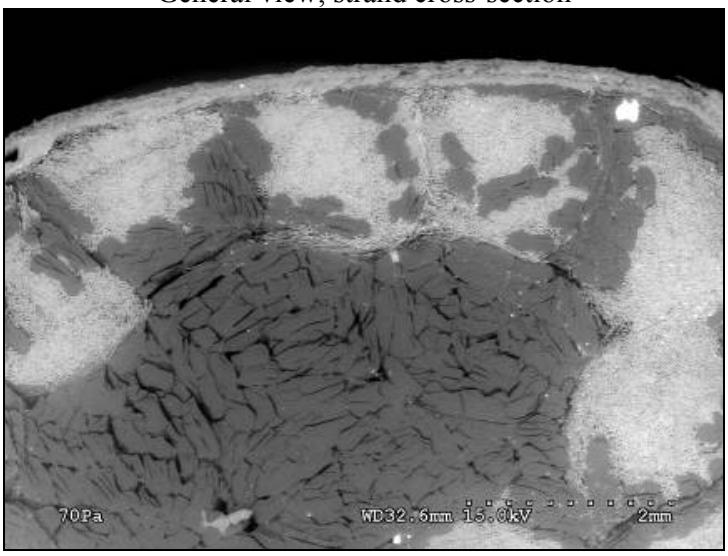

The minimum magnification of x18 was used, but the sample was too big to allow a complete view of the cross section. It can be seen however that there is an outer layer of yarns, consisting of an assembly of monofilament PP and multifilament PET. This outer layer surrounds an inner core of monofilament PP.

A very large particle is seen towards the top right of the image, and is probably entered during the sample preparation.

L1 EVERSON USED ROPE

Photograph 22 shows a general view of the outer face of the L1 used rope and Photographs 23 and 24 show further views of the outer face in greater detail.

Photograph 22 L1 Used rope

General view of outer face

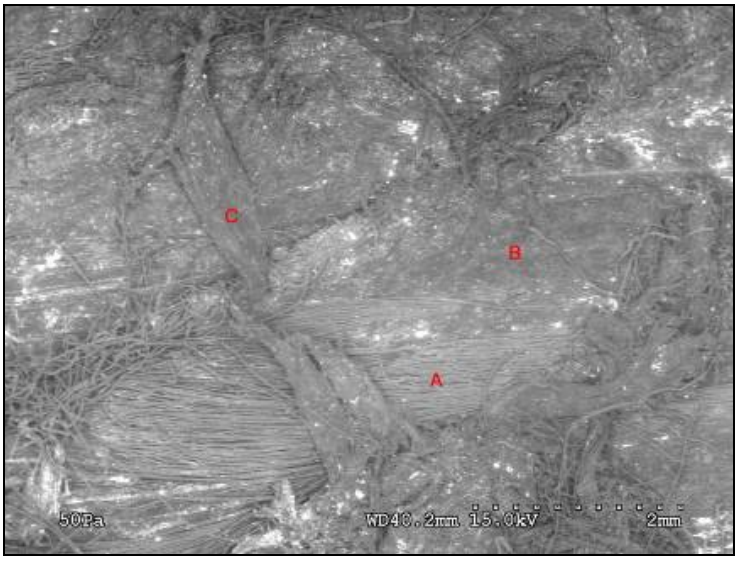

A multifilament PET yarn is seen at A [broken filament are also seen]; a monofilament PP yarn at B; and damaged monofilament at C. Particle contamination is readily seen as white areas in the image. Compared to Photograph 2, L1 machine tested outer surface, the particle contamination is greater for the used rope.

Photograph 23 L1 Used rope

Another view of damaged and contaminated outer face

Photograph 24 L1 Used rope
Flattened polyester multifilaments, outer face

Flattening is seen at A, but it is seen over the whole image. Compared to Photograph 4, L1 machine tested, the severity of flattening is less, suggesting that that the machine testing creates more pressure on the rope.

Photograph 25 L1 Used rope
Close view of inner face, ridge area

Flattened polyester filament debris embedded in fibrillated PP are seen. Particle sizes are 50 micron and less are also seen in this image.

Photograph 26 L1 Used rope General view, cross-section

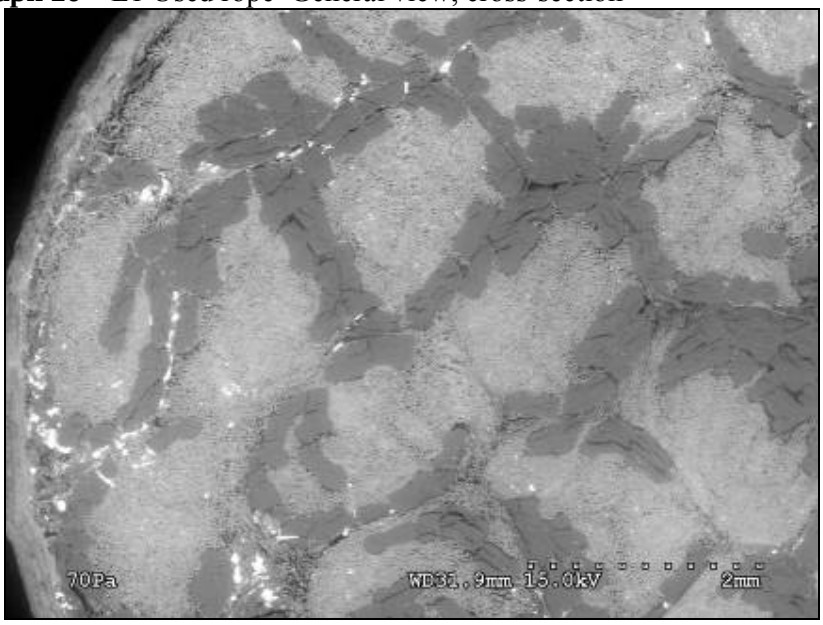

It may be seen that the strand is constructed differently from the strands used in the machine tested rope, in that there is no evidence of an inner core of monofilament PP.

In the image above, the migration path for sediment particles is seen to follow the outside of a rope yarn, where the PP monofilaments form the outer layer. Migration of particles into the multifilament PET is comparatively small.

Photograph 217 is a close view of the outer layer of the strand

Photograph 27 L1 Used rope
Close view, cross-section

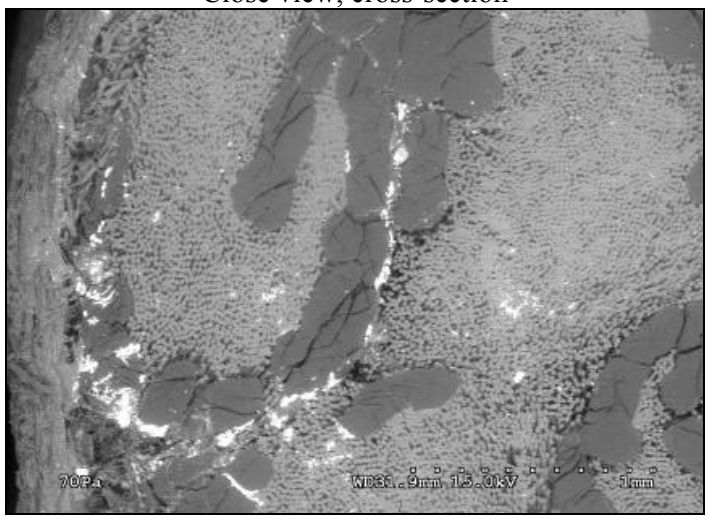

The migration path is seen, though some clusters of particles are seen within the PET filaments.

There appears to be a tendency for sediment particles to fill voids in the internal structure of the PP filaments and along the boundary. It is suggested that these voids are created by a delamination mechanism that has its origin in flex fatigue. However,

it is possible, but very unlikely, that these voids were created during sample cutting. Investigating further cross-sections made by the alternative sample preparation technique already described would remove all doubt.

The diameters of the filament components are the same as for the machine tested rope. It is difficult to determine if the sediments, seen as the white areas, are agglomerations of smaller particles, though it would be expected that this is the case.

CONCLUSIONS FROM COMPARING SEM IMAGES

The overall conclusion from this set of photographs is that, for these specimens, sediment has not played a significant role in damaging the rope. The damage seen has its origins in external mechanical abrasion and internal strand-on-strand abrasion. Evidence of damage caused by pressure was seen, particularly on the PP monofilaments. This is to be expected as polypropylene has a lower softening temperature than polyester. However, flattened PET filaments were seen, further evidence of the effect of pressure on the rope structure.

In cross section large voids were seen in the PP monofilaments. It is suspected that they have been caused by internal delamination, this being due to flex fatigue and internal pressure caused by winching or a combination thereof.

We also note that contamination within the PET filament clusters is minimal. There was little evidence to suggest damage to the PET filaments caused by particle contamination: however, this would be difficult to discern for certain looking at broken and tangled filaments.

The outer face of the machine tested rope appears to have suffered a greater degree of external abrasion. The severity of flattening of the polyester filaments also appears to be greater for the machine tested rope.

Comparing the used and machine tested ropes, a difference is seen in the degree of particle penetration, and the manner in which particles migrate within the rope. For the machine tested strands, particles appear to be dispersed within the PET filaments as well as around the perimeters of the PP filaments. For the used rope, there appears to be a distinct preference for the particles to migrate around the PP filament perimeters, and a lesser preference to migrate through the PET filaments.

The degree of particle penetration appears to be greater for the used rope.

A dominant feature of the cross sections was the tracking of sediment along the PP yarn. This maybe due to the larger gaps between and within PP yarns. To limit tracking of particles, the PP should be within the centre of the strand, surrounded by polyester, since the polyester packs more closely together and has better filtering effect.

Figures 27 through 32 provide side-by-side comparisons of machine tested and used ropes under SEM examination.

L 1

Used – Outer face

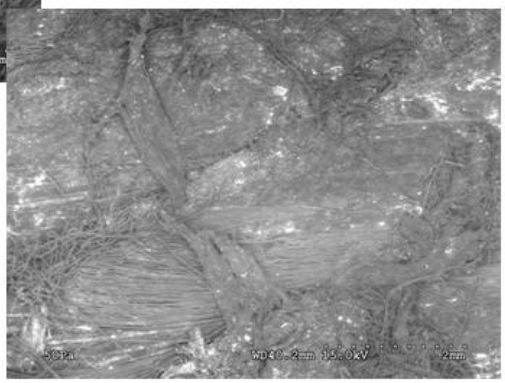

Machine tested – Outer face

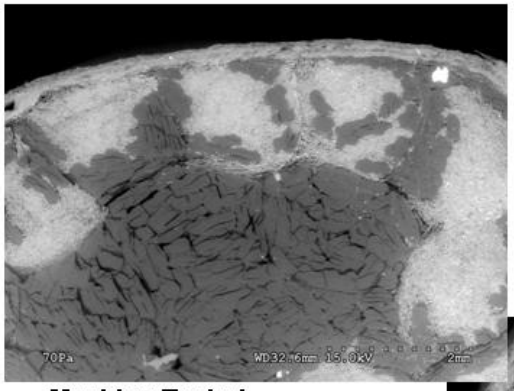

Machine Tested

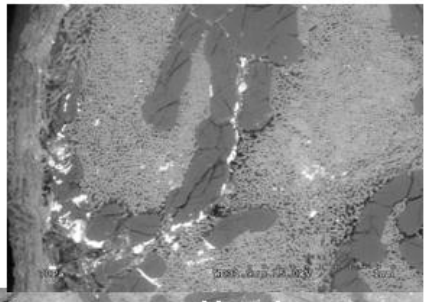

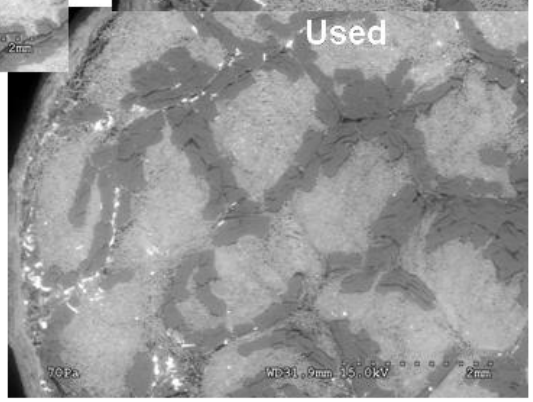

L 1

Cross sections

L 10

Machine tested - outer face

Used – outer face

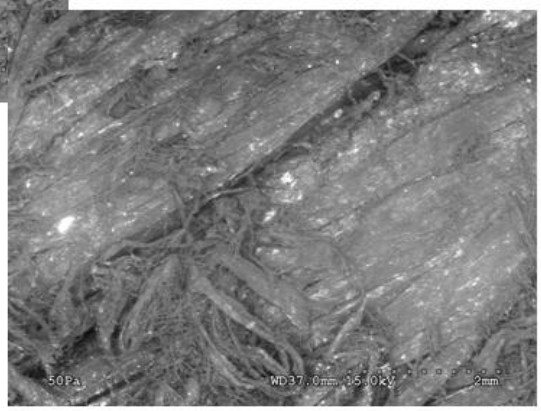

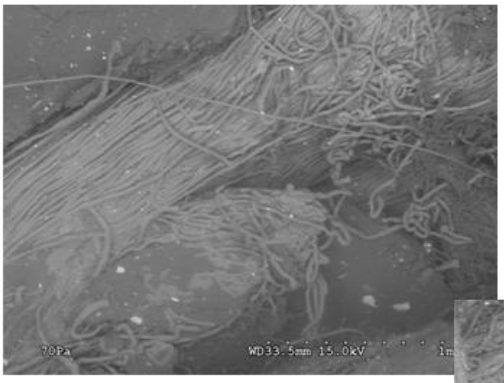

L 10

Machine tested – inner face

Used – inner face ridge

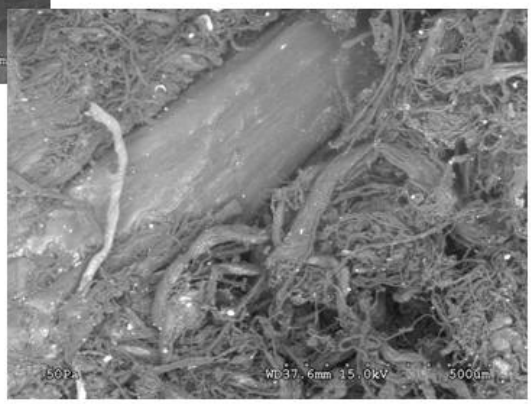

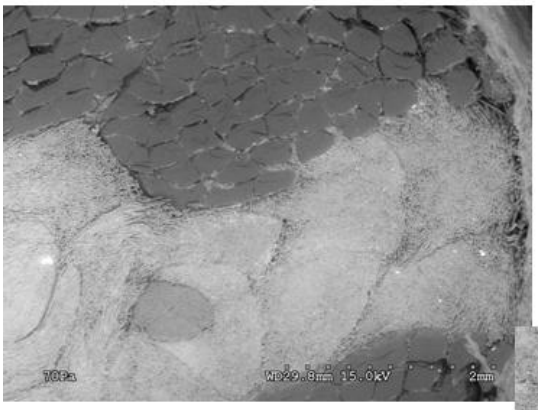

Machine tested – X section

L 10

Used – X section

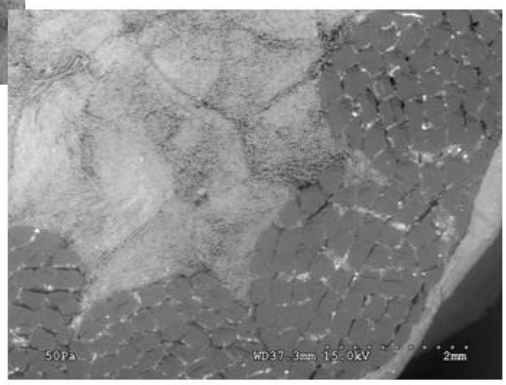

6 OVERALL CONCLUSIONS

Sediment does not appear to have a major role in the damage seen for these particular ropes, both used and machine tested .

The damage mechanisms that were most prevalent were:

1. External abrasion, most likely caused by working the ropes over winches, marginally exacerbated by sediment
2. Internal abrasion, caused by yarn-on-yarn relative movement
3. Pressure, causing flattening and breakage of the multifilament PET yarns, and flattening and softening/flowing of the PP yarns
4. Internal flex fatigue was evident on the PP monofilaments. Voids were found that suggested a de-lamination process had occurred due to differential stresses within the filament, introduced by repeated bending and/or elongation.

The testing machine appears to reproduce mechanical damage quite well, but particle migration through a rope cross-section appeared to be less for machine tested ropes than for used ropes. Ways should be found to contaminate rope with more sediment prior to machine testing.

X-Ray spectra suggest a difference between the machine sediment medium and the sediment which the used ropes had experienced.

7 RECOMMENDATIONS

The following recommendations are made for future evaluation of non-buoyant groundlines when utilizing the laboratory simulator.

1. Establish baseline data for mechanical wear by running a new rope in the simulator without sediment.
2. Place a new line on the bottom for a typical season but do not haul it. Analyze sediment ingress and test in simulator.
3. Develop a method of contaminating ropes for simulator testing that better models used ropes.
4. Prepare a rope specification, based on existing fishing industry data, that would produce a rope with good potential for durable service.
5. Procure ropes to this common specification that will be field and simulator tested over an upcoming lobstering season.